Indian Journal of Chemical Technology
Vol. 25, September 2018, pp. 441-450

Studies on corrosion inhibitory action of *Ocimum sanctum* (Tulsi) leaves extract in mild steel corrosion induced by *Desulfovibrio desulfuricans*

S Chaithra[1], Apeksha Gupta[2], R Manivannan[2] & S Noyel Victoria*[,1,2]

[1]Department of Chemical Engineering, National Institute of Technology Karnataka, Surathkal 575 025, Karnataka, India.

[2]Department of Chemical Engineering, National Institute of Technology Raipur 492 010, Chhattisgarh, India.

E-mail: snvictoria.che@nitrr.ac.in

Received 20 November 2016; accepted 26 July 2017

Studies on the effect of *Ocimum sanctum* (Tulsi) leaves extract as corrosion inhibitor for mild steel corrosion caused by *Desulfovibrio desulfuricans* has been carried out. The extract provides 74% inhibition efficiency and is effective up to two weeks. Potentiodynamic polarization studies show the occurrence of pitting corrosion. The electrochemical impedance spectroscopy studies reveal that the nature of the biofilm formed changes continuously. The scanning electron microscopy studies on samples immersed for different durations indicate two layers of different morphologies formed at the end of third and fourth weeks in the uninhibited sample. Energy dispersive x-ray diffraction studies show an increase in sulfide content in uninhibited sample indicating formation of corrosion products.

Keywords: *Ocimum sanctum*, Biocorrosion, Impedance, Polarization, *Desulfovibrio desulfuricans*

Control of the corrosion caused by microorganisms generally referred as microbially induced corrosion (MIC) or biocorrosion has gained considerable interest in recent years. Microbial activity, particularly of sulfate reducing bacteria (SRB) causes souring of oil reservoirs and corrosion of the iron and steel units in oil refineries[1]. Apart from damages caused to the plant equipment, souring impacts the quality of the oil and poses risk of H_2S toxicity[1]. Among corrosion causing microorganisms, SRB is considered to be primary corrosion causing agents because of their injurious metabolic activities which arise as a result of their ability to serve as an electron donor, use O_2 and Fe^{3+} as electron acceptor, use hydrocarbons as carbon source, combine sulfate reduction to the intracellular production of magnetite and favors elemental oxidation of iron[2]. Various techniques are in practice including mechanical pigging, application of biocides, electrochemical treatments and biological treatment by including beneficial microbial species for the control of biocorrosion[2]. Out of these practices, application of biocides is considered to be effective[2]. Biocides are group of chemical compounds capable of killing / controlling the microbial growth[3]. Some of the biocides in common use are ozone, chlorine, quaternary ammonium compounds and aldehydes[3]. These synthetic biocides are expensive and potentially harmful to the environment[4]. Hence, the current focus is on inexpensive environmentally safe biocides which are extracted from plants called as green inhibitors[4]. The plant extracts contain polar functional groups with sulfur, nitrogen and oxygen atoms in their molecule, heterocyclic compounds and π electrons which are believed to be responsible for their corrosion inhibition properties[5]. Though green inhibitors have been studied extensively for chemicals induced corrosion on many metals, their application to control the biocorrosion is less reported[6]. Neem leaf extract was reported to have corrosion inhibition property against the MIC caused by SRB in pipeline steel[2]. Extracts of *Brassica nigra, Allium sativum, Allium cepa and Zingiber officinale* have been studied for their corrosion inhibition properties against MIC[6,7]. The extracts from *Ocimum sanctum* have been found to give good corrosion protection and was also claimed to have good antibacterial property[8,9].

The present work investigates the use of *Ocimum sanctum* (Tulsi) leaves extract as corrosion inhibitor for MIC caused by *Desulfovibrio desulfuricans* species in mild steel (MS) specimen. The effectiveness of the extract in the control of MIC induced by *Desulfovibrio desulfuricans* species was studied using weight loss and electrochemical characterization studies. The morphology of the samples immersed in media with and without inhibitor was analyzed using scanning electron microscopy (SEM). The chemical composition of the

surfaces was investigated using energy dispersive X-ray analysis (EDAX) and Fourier transform infrared spectroscopy (FTIR) studies.

Experimental Section

Culturing the organisms

Pure freeze dried samples of *Desulfovibrio desulfuricans* was obtained from National Collection of Industrial Microorganisms (NCIM), Pune. The strains were cultivated in a medium containing dipotassium phosphate (2 g/L), magnesium sulfate (0.1 g/L), calcium chloride (0.1 g/L), ammonium sulfate (0.1 g/L), ferric chloride (0.02 g/L) and sodium thiosulphate (10 g/L). This nutrient medium was sterilized at 1.5 kg/cm^2 gauge pressure for 20 min in an autoclave. Before use, the medium was bubbled with nitrogen to remove the dissolved oxygen. The medium was then filled into amber colored test tubes with caps to which *Desulfovibrio desulfuricans* were added. The tubes were incubated in dark place at 37°C. The sulfide content was analyzed periodically by titration method[10]. The sulfide estimation was performed to find out the stationary growth phase period for the *Desulfovibrio desulfuricans*.

Preparation of the plant extract

Leaves of *Ocimum sanctum* (Tulsi) were washed, shade dried for 3 days, followed by tray drying at 50-60°C for 2 hr and then grinded. The powder was soaked in ethanol for 24 hr and was refluxed for 5 hr at 55°C. Once the contents reached the room temperature, the solution was filtered and concentrated using vacuum evaporator. The concentrated extract was used for further studies.

Weight loss experiments

Mild steel coupons with composition of 0.099 wt% C, 99.3 wt% Fe, and trace amounts of Ni, Cr, P, Si were used for the studies. The dimension of the mild steel coupons used for the studies was 10 mm × 10 mm × 0.5 mm. Mild steel coupons were polished with different grades of sand paper washed with acetone and distilled water and stored in desiccator. Prior to use the coupons were washed with ethanol. The autoclaved nutrient medium was filled into the test tubes and the pre-weighed coupons were immersed into the test tubes. The tube with nutrient medium without inhibitor extract and SRB culture in it is referred as blank. The mild steel coupons immersed in blank were immersed for 28 days and at the end of the immersion period the weight loss was calculated. Mild steel coupons immersed in the medium containing SRB without inhibitor extract are referred using the name uninhibited sample while those immersed in the medium with SRB and inhibitor extract are referred as inhibited samples. The weight loss of the inhibited and uninhibited samples was measured every week for four consecutive weeks and was used for corrosion rate (*CR*) calculation. The *CR* can be calculated using the equation 1

$$CR = \frac{W \text{ x } 8.76 \text{ x } 10^4}{\rho A t} \quad \text{... (1)}$$

where *CR* is the corrosion rate in mm y^{-1}, *W* is the weight loss in g, ρ is the density of the metal in g cm^{-3}, *A* is the area of the sample in cm^2 and *t* is the immersion period in h.

Electrochemical measurements

The electrochemical experiments were conducted in an electrochemical workstation (CH609IE, CH instruments, USA). A three electrode setup with the immersed mild steel sample as the working electrode, Ag/AgCl as the reference electrode and platinum counter electrode was used. Prior to potentiodynamic polarization and electrochemical impedance spectroscopy (EIS) runs, a stabilization period of 30 min was given. The potentiodynamic polarization studies were run at a scan rate of 1 mV s^{-1} with a potential range of ± 250 mV with respect to open circuit potential (OCP). The EIS runs were performed between the frequency range 100 kHz and 0.1 Hz with 10 mV rms amplitude for the alternating current (AC) signal. The potentiodynamic polarization plots were analyzed for E_{corr} and I_{corr} using the CH609IE software and Zsimpwin was used to analyze the EIS data.

Results and Discussion

The sulfide content of the medium with SRB culture in different intervals of time was measured. The sulfide content after 48 hr and 72 hr were measured as 19.4 ppm, and 19.5 ppm respectively. Maximum of 22.6 ppm sulfide content was observed at 96 hr. After 96 hr, the sulfide content decreased slightly to 20 ppm and remained stable at 20 ppm till 168 hr. The sulfide content shows that the SRB reaches growth phase in 48 hr to 96 h duration and reaches stationary phase after 96 hr. Weight loss results match well with the sulfide analysis. The corrosion rate was maximum in the first week, at which the bacteria are in stationary phase. After first week, the increase in sulfide concentration, shortage of nutrients causes a decrease in the bacterial population resulting in decreased corrosion rate.

Weight loss experiments

Table 1 shows the inhibition efficiencies offered by different concentrations of *Ocimum sanctum* leaves extract for 4 weeks immersion period. It is seen that the inhibition efficiency is high for 2 vol% extract concentration. Hence, 2 vol% concentration was used for all the studies. It can be clearly seen that the blank nutrient medium without bacterial culture was able to cause corrosion of mild steel. The corrosion rate of mild steel in blank at the end of four weeks was 0.01 mm y^{-1}. The corrosion rate of the mild steel in contact with medium with SRB culture was 0.06 mm y^{-1}. On the other hand, the media with bacterial culture in the presence of different concentrations of tulsi leaf extract, showed a corrosion rate from 0.01 to 0.02 mm y^{-1} upon four week immersion. Thus it is clear that the extract is effective in controlling the growth of the SRB, however the corrosive action of the medium is not controlled which results in similar corrosion rate values as that of the blank medium without SRB culture and extract. Thus, the tulsi leaf extract acts as a good bactericidal agent stopping the growth of the bacteria, but a weak corrosion inhibitor to prevent corrosion due to the nutrient medium.

Potentiodynamic polarization

Figure 1 show the potentiodynamic polarization curves for mild steel coupons immersed medium with and without 2 vol% inhibitor for different durations respectively. The Tafel parameters were obtained by linear extrapolation of the Tafel plots and are presented in Table 2. It is clearly seen from the Fig. 1 that with increase in immersion time the cathodic exchange current density increases and the anodic exchange current density decreases. The E_{corr} values shows significant shift in the positive direction. Such a trend under anaerobic conditions is an indication of bacterial catalysis of the cathodic reaction[11]. The positive shift in the E_{corr} value is referred as ennoblement which is claimed to be the result of formation of film due to bacterial activity[6]. Literature states that the SRB reduce the sulfates to hydrogen sulfide (H_2S) and gain energy

Table 1 — Effect of inhibitor concentration on the inhibition efficiency.

Inhibitor concentration (vol %)	Weight loss (mg)	Inhibition efficiency (%)	*CR* (mm/y)
0	3.38	-	5.6×10^{-2}
1	1.2	63	2×10^{-2}
2	0.88	74	1.5×10^{-2}
3.5	0.99	71	1.6×10^{-2}

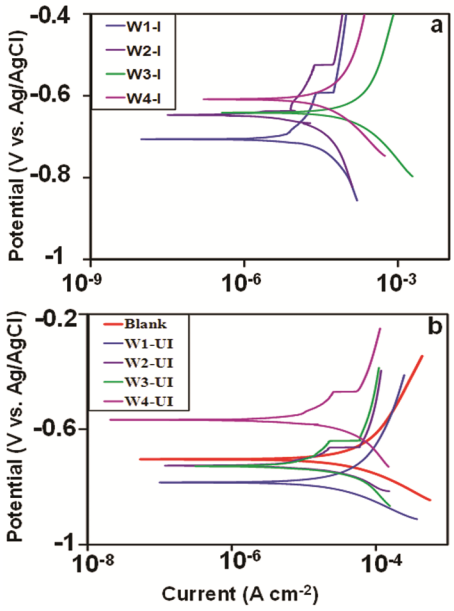

Fig. 1 — Potentiodynamic polarization plots for the mild steel coupons in different medium at different immersion periods a) with 2 vol% inhibitor extract b) without inhibitor extract and blank.

Table 2 — Electrochemical parameters from potentiodynamic polarization studies for mild steel immersed in different medium for different immersion periods

Immersion period (weeks)	Medium	β_a (mV dec^{-1})	β_c (mV dec^{-1})	I_{corr} (μA/cm^2)	R_p (kOhm/ cm^2)	E_{corr} (V)
1	Uninhibited	220	90	31	0.89	-0.78
	Inhibited	110	155	12	2.33	-0.68
2	Uninhibited	110	90	17	1.26	-0.73
	Inhibited	200	210	13	3.42	-0.64
3	Uninhibited	200	230	27	1.72	-0.62
	Inhibited	310	160	83	0.55	-0.64
4	Uninhibited	140	180	22	1.55	-0.52
	Inhibited	120	140	21	1.34	-0.61
4	Blank	243	160	42	1.00	-0.7

for their growth. Recent studies have proposed only metal plays the role of electron donor[12,13] and thus corrosion is a result of biological catalysis and not a result of abiotic cathodic effect[12]. The observed ennoblement and the increase in cathodic exchange current density in the case of MS coupons immersed in medium without inhibitor is considered to be due to the direct electrical coupling of the initial iron dissolution reaction in combination with biological reduction of sulfate which emerges as the dominant cathodic reaction[12]. The iron dissolution results in the release of electron as shown by reaction 2[12].

$$Fe^{2+} + 2e^{-} \leftrightarrow Fe \quad \ldots (2)$$

The electrons thus liberated are consumed according to the direct electron uptake by the SRB resulting in electrical microbially influenced corrosion (EMIC) by the attached SRB cells shown in reaction 3[12].

$$8e^{-} + SO_4^{2-} + 10H^{+} \rightarrow H_2S + 4H_2O \quad \ldots (3)$$

The overall reaction between iron, H_2S and carbonates which are available in traces can be given by reaction 4 resulting in the formation of precipitates of iron salts which is a part of the biofilm [12,14].

$$4Fe + SO_4^{2-} + 3HCO_3^{-} + 5H^{+} \rightarrow FeS + 3FeCO_3 + 4H_2O \quad \ldots (4)$$

The MS coupons in medium with inhibitor also exhibits ennoblement, however the magnitude of the same is much lower than the uninhibited one. From the weight loss results it is seen that the corrosion inhibition is not 100% achieved, the inhibition efficiency of maximum 74% was achieved. This matches well with the potentiodynamic polarization results. Following the corrosion current I_{corr} values under different conditions show that the I_{corr} values are significantly lower in the medium with inhibitor for the first two weeks. This could be due to the inhibitor molecules effectively controlling the growth of the microbes. In the third week the I_{corr} values are higher when compared to the uninhibited case which can be explained by the loss in the inhibition activity of the molecules to minimize corrosion. The I_{corr} values of the fourth week in both the cases are closer which could be due to the combined action bacteria reaching death phase and formation of the biofilm. The samples which were immersed in blank nutrient medium without inhibitor and SRB culture showed an I_{corr} value of 42 μA after 4 weeks of immersion which is higher than the I_{corr} values of uninhibited and inhibited samples immersed for same period. In the case of uninhibited samples this smaller I_{corr} value is attributed to the presence of biofilm formed by the biological action and bacteria reaching the death phase. In inhibited medium, it is due to inhibitor activity in control of bacterial population. The R_P value was calculated from the cathodic (β_c) and anodic (β_a) Tafel slopes using the Stern Geary equation shown in equation 5[6].

$$R_P = \frac{\beta_a \beta_c}{2.3(\beta_a + \beta_c) I_{corr}} \quad \ldots (5)$$

The R_P values match well with the corrosion current. Except for the third week, the uninhibited sample exhibits higher resistance to corrosion.

Electrochemical impedance spectroscopy

The reliability of EIS data can be ensured using Kramers Kronig Transformation (KKT)[4,6]. If a data set obeys KKT, then the system which belong to those data set is believed to be stable, linear and causal[4,6]. The system was found to obey KKT (not shown here) and thus was found to be stable. The Bode plots of Z moduli with frequency for the inhibited and uninhibited systems are shown in Figs. 2a and 2b, the high frequency region from 10^5 Hz to 10^2 Hz presents a horizontal asymptote which is characteristic of resistive behavior[15]. From Fig. 2a and 2b it is clear that the impedance values increase with immersion time in both inhibited and uninhibited cases. In the low frequency region the Z moduli vs. frequency does not show the presence of horizontal asymptote which is indicative of diffusion

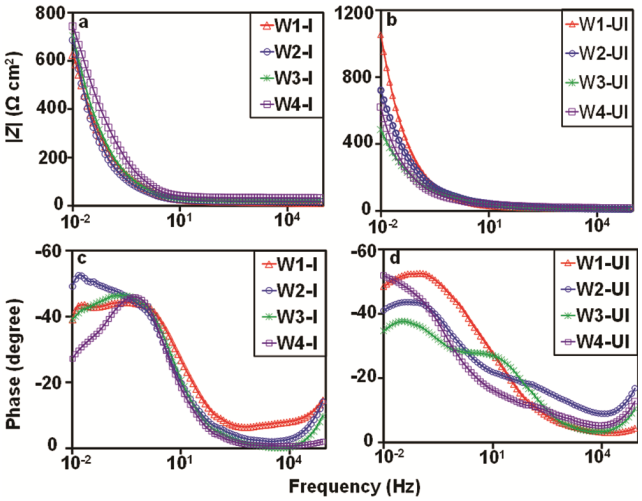

Fig. 2 — Bode plots for the mild steel coupons in different medium at different immersion periods. a) | *Z* | vs. frequency for inhibited sample b) | *Z* | vs. frequency for uninhibited sample c) Phase vs. frequency for inhibited sample d) Phase vs. frequency for uninhibited sample.

limitation[15]. The Bode phase plot Figs. 2c and d shows the phase angle approaching 45° at lower frequencies[15]. The asymmetric nature of the phase angle peak at lower frequencies shows the presence of two time constants[16]. The Nyquist plots for uninhibited and inhibited system shown in Fig. 3a and 3b respectively show depressed semicircle indicating frequency dispersion caused by rough and heterogeneous surfaces[4]. Hence, constant phase element (CPE) has been considered for modeling capacitive behavior. A CPE can be expressed mathematically using equation 6.

$$Z_{CPE} = \frac{1}{Q_i (j\omega)^{n_i}} \quad \ldots (6)$$

Where Z_{CPE} is the impedance of the CPE, Q_i is the proportionality constant, ω is the angular frequency and n_i is the surface roughness parameter[4]. An electrical equivalent circuit (EEC) as shown in Fig. 3a and 3b (inset) has been used to study the system. In Fig. 3a and 3b, R_s represents the solution resistance, R_1CPE_1-the first relaxation process characterizes the surface layer formed by the deposition of corrosion products and biofilm[15]. The second relaxation process R_2CPE_2 represents the double layer capacitance. The external surface layer is believed to be formed by the deposition of corrosion products, adsorption of the inhibitor molecules and biofilm. Hence, it is considered to be a rough heterogeneous structure which is less compact. A less dense rough structure can provide diffusion passages and Warburg impedance (W) is an appropriate element to model such semi-infinite length diffusion[15,17]. Warburg impedance (W) is commonly used diffusion element for semi-infinite cases. The general representation for W is given by equation 7.

$$Y(W) = Y_0 (j\omega)^{1/2} \quad \ldots (7)$$

where Y_0 is the diffusion coefficient. The equivalent capacitance for the external layer and the double layer can be calculated from the CPE parameters using the equation 8[6].

$$C_i = (Q_i \; R_i^{(1-n_i)})^{1/n_i} \quad \ldots (8)$$

where, R_i is the resistance associated with the individual CPE. The relaxation time constant (τ_i) can be calculated using the equivalent capacitance from equation 9[6].

$$\tau_i = C_i \; R_i \quad \ldots (9)$$

The polarization resistance R_P can be calculated from the sum of R_1 and R_2. The values of the EEC fit parameters are presented in Table 3. It is seen from Table 3 that the R_p value for the inhibited sample increases significantly upon two weeks immersion time which decreases further for third and four weeks of immersion. The higher R_p upon two weeks immersion can be attributed to the adsorption of the inhibitor molecules, external surface layer formed by corrosion products and biofilm. The I_{corr} values from the potentiodynamic polarization studies are lower for first two weeks in inhibited samples. These observations indicate that the inhibitor extract helps in minimizing the corrosion rate by controlling the bacterial activity and by adsorption on to the surface of the metal. However, the extract is not effective in offering control over corrosion beyond two weeks which is reflected by decreasing R_p values for subsequent weeks and increase of I_{corr} values in the third week. This loss in

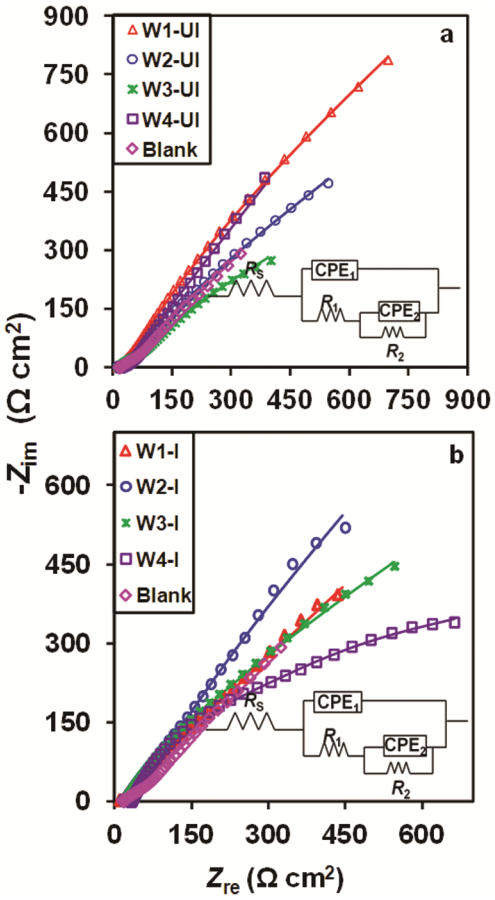

Fig. 3 — Nyquist plots for the mild steel coupons in different medium at different immersion periods. a) Uninhibited sample b) Inhibited sample. The line represents EEC fit for the experimental data. The inset figure represents the corresponding electrical equivalent circuits.

corrosion control capacity of the inhibitor could be due to desorption of the inhibitor molecules and weakening of the external layer formed on the metal surface. The uninhibited case on the other hand, shows maximum R_p at the end of first week which further decreases for the subsequent immersion periods. A high R_p value of the first week could be due to the increased number of viable bacterial population and formation of the biofilm. The living bacterial cells are not conductive when compared to dead ones which are conductive in nature[6,18]. Hence the extent of corrosion can be expected to be high during the first week. This is supported by the higher I_{corr} value for the uninhibited case in potentiodynamic polarization studies. The continuous drop in R_p with prolonged immersion time could be due to the breakdown of the biofilm caused by the colonization of the bacteria and propagation of pitting corrosion[6,19]. However, the potentiodynamic polarization studies on uninhibited sample immersed for three weeks show an I_{corr} value which is lower than the inhibited sample immersed for same duration. This could be due to the protective effect of the biofilm with inactive bacteria. The equivalent capacitance (C_i) values of the layers give useful information on the thickness of the films formed on the metals coupons which is given by equation 10[6].

$$d_i = \frac{\varepsilon_0 \varepsilon_i A_i}{C_i} \quad \text{... (10)}$$

In equation10, d_i is the thickness of the film, ε_0 is permittivity of free space and ε_i is dielectric constant of the film and A_i is the total exposed area[6]. When the product of all the parameters in the numerator of equation 10 is considered constant, C_i can be considered to be inversely related to the thickness of the film, d_i. The capacitance values were found to be many orders higher than the commonly observed values. Such higher values however, are frequently encountered in biocorrosion[6,12,19]. One of the reasons for such uncommon capacitance values in some bacteria could be due to the pseudo-capacitance caused by the c-cytochromes present on the outer cell membrane[6,20]. A higher capacitance value indicates that the products formed of corrosion process are conductive and the layer is porous[12,21]. In biocorrosion and biofilms, the interpretation of the C_i values needs a comparison with results from other studies. A very low C_f value for first week inhibited sample indicates a thicker outer layer formed by the corrosion products and biofilm which is relatively less porous and non-conductive[19,22,23]. A very low I_{corr} value for the first week inhibited sample from potentiodynamic polarization studies supports this view. A significant increase in the C_f value for the second week inhibited sample could be due to desorption of some of the adsorbed inhibitor molecules and damage caused to the external layer.

Further, unstable trend in the C_f values indicate the unstable nature of the external layer[24]. The C_{dl} values corresponding to the double layer of the solution-metal interface of the inhibited samples increase significantly with immersion period which indicate an accumulation of charge[24]. In uninhibited sample the

Table 3 — EEC fit parameters for mild steel coupons immersed in different medium for different immersion periods

Parameters	Inhibited				Blank	Uninhibited			
	W1	W2	W3	W4	W4	W1	W2	W3	W4
R_S (Ω cm^2)	5.6	16.8	20.8	31.4	15	14.4	12.3	14.3	18.3
$10^3 Q_1$ (S s^n/ cm^2)	1.6	6.2	3.3	2.9	6.9	3.7	2.6	3.2	2.3
n_1	0.3	0.6	0.8	0.7	0.4	0.6	0.5	0.6	0.5
R_1 (Ω cm^2)	13	722	152	552	307	243	83	141	32
$10^3 Q_2$ (S s^n/ cm^2)	2.1	3.8	3.9	11.7	3.6	1.2	3 .2	6.8	5.6
n_2	0.8	0.9	0.6	0.9	0.8	0.8	0.6	0.7	0.6
R_2 (kΩ cm^2)	0.1	1.3	1	0.2	0.9	3	2.4	0.6	0.5
10^3 W-Y_0 (S s$^{0.5}$/ cm^2)	3	2.6	6.2	14.4	0.8	2.4	3.6	11.5	0.3
C_1 (μF/ cm^2)	1.2	14363	2756	3542	17847	3592	479	1753	211
C_2 (μF/ cm^2)	1532	3918	10131	12840	4238	1739	8074	11313	11776
τ_1 (s)	0.00001	10	0.4	2	5	0.8	0.03	0.2	0.007
τ_2 (s)	0.1	5	10	4	4	5	19	7	7
R_p (kΩ cm^2)	0.1	2	1	0.8	1	3	2	0.7	0.6

C_f value which signifies external layer shows maximum on two weeks immersion. This high C_f value could be due to the conductive layer of Fe_xS_y formed by bacterial activity and damage to the biofilm[21]. A value of 0.6 for roughness factor and slight increase in the corrosion current from potentiodynamic polarization studies support this. The C_{dl} values of uninhibited sample show increasing trend with immersion time along with continuously decreasing R_{ct} which indicates an increase in charge accumulation due to the growth of biofilm[25,26]. The R_p values for the inhibited samples increases upto two weeks and decreases for the subsequent weeks. The magnitude of R_p for the uninhibited samples is lower when compared to the inhibited sample indicating lesser corrosion. The sample immersed for four weeks in medium without bacterial culture and inhibitor showed slightly higher R_p indicating lower corrosion rate. The R_p values calculated from potentiodynamic polarization studies differ slightly from the values calculated from EIS parameters. Such mismatch is often observed in biocorrosion[6]. The use of β_a and β_c Tafel slopes to calculate R_p form Stern Geary relation leads to over estimation of R_p when the potentiodynamic polarization shows deviation close to the corrosion potential[6]. The R_p values of the inhibited samples show maximum in the second week, indicating a thicker outer layer formation due to the adsorption of the inhibitor molecules, biofilm and corrosion products deposition. The R_p values decrease for the third and fourth weeks of immersion which shows unstable nature of the film. The R_p value of the uninhibited samples present a decreasing trend with immersion time with maximum value in the first week. This could be due to the increase in dead bacterial cells which are highly conductive and accumulation of corrosion products[6]. The relaxation time constant is a measure of time required for return of charge distribution to equilibrium after an electric disturbance[27]. The fluctuating values of τ_i indicate unstable nature of the system because of the changes taking place at the outer layer[28]. The τ_f values for the inhibited sample shows a maximum in the second week indicating slower adsorption[29]. The magnitude of τ_f values of the uninhibited samples is smaller when compared to inhibited samples. The parameter Y_0-W is related to diffusion layer. For inhibited samples, Y_0-W decreases for two weeks immersion and increases for third and fourth weeks. The increased Y_0-W value with increased immersion time accompanied with decrease in resistance indicates increase in the area available for corrosion[17]. Whereas, in the case of uninhibited samples, the Y_0-W continuously increases for three weeks which drops for the fourth week which could be due to the formation of biofilm.

Scanning electron microscopy

Figure. 4 (a-f) shows the morphology of the samples immersed for different durations in medium with and without inhibitor extract analyzed using scanning electron microscopy. Figure 4 (a-d) shows the surface of the samples immersed in uninhibited medium for 7, 14, 21 and 28 days respectively. It is seen that the surface of the coupons immersed in uninhibited medium for one week show the presence of densely distributed flaky structure, which could be formed of corrosion products. Such features were also reported in the SRB corrosion of carbon steel[21]. For the second week sample, the density of the crystallite corrosion products has decreased with the appearance of tiny globular structures which could be due to the biofilm formation. The third week sample shows the presence of tiny globular amorphous structures with high porosity covering the crystalline corrosion products completely. The fourth week uninhibited sample also shows the presence of globular structures amorphous structures completely covering the crystalline features. These amorphous globular/ fibrous structures could be due to the biofilm formation due to the bacterial activity. The fourth week inhibited sample on the other hand shows the presence of clear crystalline features densely covering the sample. This could be due to the layer formed by the deposition of corrosion products and inhibitor molecules. The fourth week inhibited sample does not show the presence of any biological activity or biofilm formation. The EDAX results for different samples are shown in Table 4. It is seen that the uninhibited sample shows high sulphide content when compared to inhibited ones. The uninhibited sample shows the presence of calcium for the third and fourth week samples which could be due to the precipitation of calcium salts particularly carbonates[30]. The consumption of sulfates by the SRB cause increase in sulfide content which changes the *p*H of the medium resulting in calcium salts precipitation[30]. The phosphorus present in the uninhibited samples for third and fourth week is more when compared to other samples. The increased phosphorus content could be due to biofilm growth. Phosphorus is one of the important constituent of extracellular polymeric substances which constitute the biofilm[6,31]. Presence of

calcium in the uninhibited samples of third and fourth weeks is due to the calcium binding capacity of the SRB which causes calcium carbonate precipitation in the biofilm[32]. The inhibited sample shows the presence of iron oxides. From the electrochemical studies and weight loss measurements it is observed that the tulsi leaf extract works moderately to control the corrosion up to 70%. The varying values of capacitance in both the cases indicate the change in the nature of the film formed on the surface of the samples which also matches with the observed trend.

Table 4 — Elemental composition of the coupons immersed in medium with and without 2 vol% inhibitor at different immersion periods

Elements	Weight %				
	W1-UI	W2-UI	W3-UI	W4-UI	W4-I
C	10.3	3.9	14.6	16.9	8.4
N	3.8	2.6	-	-	-
O	36.8	39.2	37.3	28.6	40.1
Mg	2.2	5.5	0.47	2.9	3.2
P K	7.7	8.5	10.9	12.8	9.9
K	-	-	3.5	1.5	-
S	5.0	1.9	4.5	2.9	0.83
Fe	34.1	38.4	15.2	27.6	37.5
Ca	-	-	13.4	6.7	-

FTIR studies

Figure 4f shows the FTIR spectrum of the inhibited and uninhibited samples. It is clearly seen that for the inhibited samples the intensity of the peaks are low when compared with the inhibited ones. Addition of inhibitor has resulted in disappearance of many peaks along with shift in the position of few peaks. Such peak shifting is attributed to the interaction between the inhibitor molecules and the metal surface[33]. Peaks in between 3500 and 3800 cm^{-1} correspond to the hydroxyl group from water molecules. The peaks corresponding to aldehyde has shifted from 1715 to 1700 cm^{-1} upon inhibitor addition. The peaks at 1540,

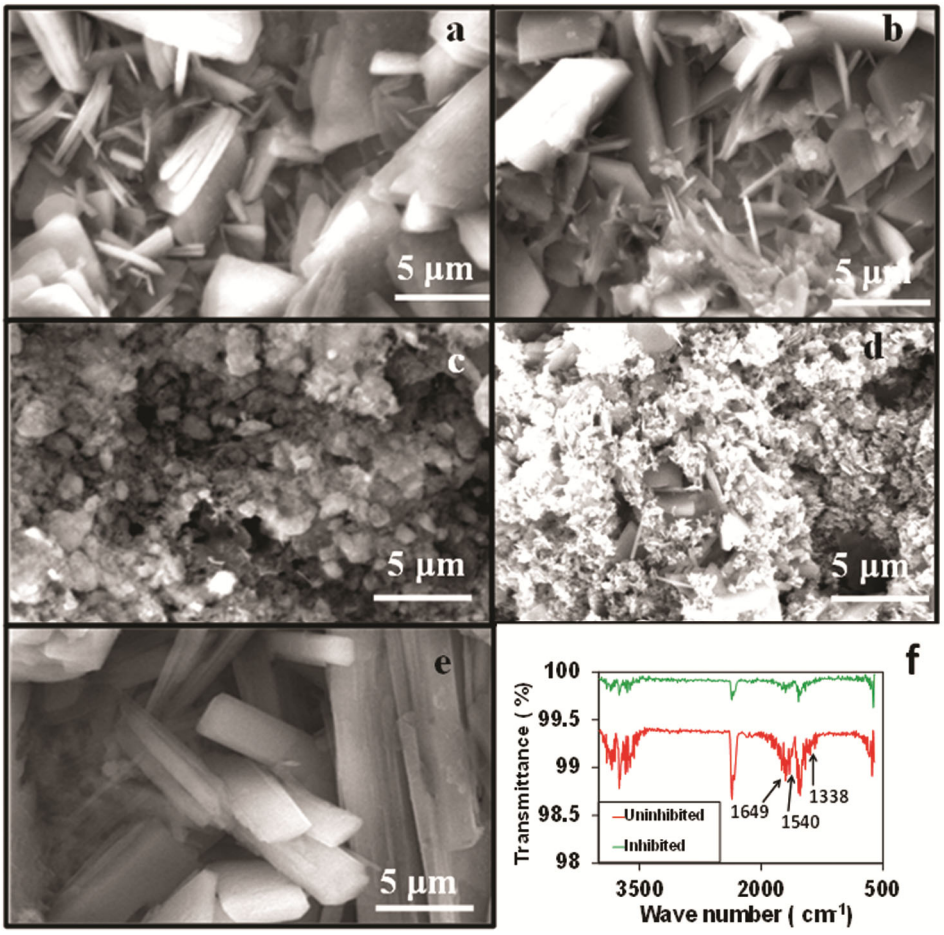

Fig. 4 — SEM images for the mild steel coupons in different medium at different immersion periods. a) first week uninhibited b) second week uninhibited c) third week uninhibited d) fourth week uninhibited e) fourth week inhibited and f) FTIR spectra of mild steel coupons in inhibited and uninhibited medium.

1338 and 1556 cm^{-1} correspond to the presence of nitro compounds such as amino acids, proteins which could have come from bacterial activity[34,35]. The peaks at 1649, 1683 and 1699 cm^{-1} correspond to the carbonyl groups[36,37].

Mechanism

Desulfovibrio desulfuricans belongs to the group of SRB. The SRB have been mentioned to cause corrosion of the metals by many mechanisms[2]. The SRB have the ability to use Fe^{3+} as electron acceptor, use aliphatic and aromatic hydrocarbons effectively as carbon source. Further along with sulfate reduction they promote intracellular magnetite production causing elemental oxidation of iron[2]. The potentiodynamic polarization studies suggest the occurrence of initial iron dissolution reaction along with bacterial sulfate reduction reaction[12]. The electrons thus released by iron oxidation are consumed by the SRB resulting in sulphates reduction which results in corrosive sulfides as shown in reactions 2 and 3. The sulfide reacts with iron resulting in iron sulfide as shown in reaction 4[12]. The sulfide content increase can be observed in uninhibited samples from EDAX analysis.

Conclusion

The effect of *Ocimum sanctum* (Tulsi) extract on the corrosion induced by *Desulfovibrio desulfuricans* on mild steel has been studied. The weight loss studied with 2 vol% inhibitor extract results in inhibition efficiency of 74% for an immersion period of 28 days. It is found that the inhibitor extract is effective in controlling the corrosion and the bacterial activity for two weeks period. The potentiodynamic polarization studies present a positive shift in the E_{corr} values which is an indication of bacterial catalysis of cathodic reaction. The analysis of the EIS results with EEC show the unstable nature of the biofilm formed in both inhibited and uninhibited samples. Scanning electron microscopy results of the uninhibited samples show the significant growth of biofilm covering the corrosion products layer for the third and fourth week samples. The EDAX results show an increased sulfur concentration in the uninhibited samples. FTIR studies support the findings of both SEM and EDAX analysis indicating the changes in the functional groups on the inhibited and uninhibited samples.

References

1 Hubert C, Nemati M, Jenneman G & Voordouw G, *Appl Microbiol Biotechnol,* 68 (2005) 272.

2 Bhola S M, Alabbas F M, Bhola R, Spear J R, Mishra B, Olson D L & Kakpovbia A E, *Eng Fail Anal,* 36 (2014) 92.

3 Videla H A, *Int Biodeterior Biodegrad,* 49 (2002) 259.

4 Victoria S N, Prasad R & Manivannan R, *Int J Electrochem Sci,* 10 (2015) 2220.

5 Yaro A S, Khadom A A & Wael R K, *Alexandria Eng J,* 52 (2013) 129.

6 Swaroop B S, Victoria S N & Manivannan R, *J Taiwan Inst Chem Eng,* 64 (2016) 269.

7 Guiamet P S & Gomez de Saravia S G, *Latin Am Appl Res,* 35 (2005) 295.

8 Kumpawat N, Chaturvedi A & Upadhyay R K, *Res J Chem Sci,* 2 (2012) 51.

9 Subramanian G, Tewari B B & Gomathinayagam R, *AIJCR,* 4 (2014) 149.

10 Kolthoff I M, Sandell E B, Meehan E J & Bruckenstein S, *Quantitative Chemical Analysis* (Macmillan, New York) 1969, 258.

11 Urquidi-Macdonald M & Macdonald D D, in *Understanding Biocorrosion: Fundamentals and Applications,* edited by Liengen T, Feron D, Basseguy R, Beech I B (Woodhead Publishing in Materials, Amsterdam) 2014, 253.

12 Venzlaff H, Enning D, Srinivasan J, Mayrhofer K J, Hassel A W, Widdel F & Stratmann M, *Corros Sci,* 66 (2013) 88.

13 Dinh H T, Kuever J, Mussmann M, Hassel A W, Stratmann S & Widdel F, *Nature,* 427 (2004) 829.

14 Starosvetsky D, Starosvetsky J, Armon R & Ein-Eli Y, *Corros Sci,* 52 (2010) 1536.

15 Finsgar M, Uzunalic A P, Stergar J, Gradisnik L & Maver U, *Sci Rep,* 6 (2016) 26653.

16 Lu Y, Dong J & Ke W, *J Mater Sci Technol,* 31 (2015) 1047.

17 Liu C, Bi Q & Matthews A E, *Corros Sci,* 43 (2001) 1953.

18 Zhai X, Ma X, Myamina M, Duan J & Hou B, *J Solid State Electrochem,* 19 (2015) 2213.

19 Belkaid S, Ladjouzi M A & Hamdani S, *J Solid State Electrochem,* 15 (2011) 525.

20 Sekar N & Ramasamy R P, *J Microbiol Biochem Technol,* (2013) S6 (2013) doi:10.4172/1948-5948.S6-004.

21 Duan J, Wu S, Zhang X, Huang G, Du M & Hou B, *Electrochim Acta,* 54 (2008) 22.

22 Wang H, Hu C, Hu X, Yang M & Qu J, *Water Res,* 46 (2012) 1070.

23 Wang H, Wang Z, Hong H & Yin Y, *Mater Chem Phys,* 124 (2010) 791.

24 Chirea M, *Catalysts,* 3 (2013) 288.

25 Sanchez-Herrera D, Pacheco-Catalan D, Valdez-Ojeda R, Canto-Canche B, Dominguez-Benetton X, Dominguez-Maldonado J & Alzate-Gaviria L, *BMC Biotechnology,* 14 (2014) 102.

26 Anandkumar B, George R P, Kamaraj K, Parvathavarthini N & Mudali U K, *T Indian I Metals,* 70(4) (2017) 1075.

27 Moradi M, Duan J & Du X, *Corros Sci,* 69 (2013) 338.

28 Castaneda H & Benetton X D, *Corros Sci,* 50 (2008) 1169.

29 Khadiri A, Ousslim A, Bekkouche K, Aouniti A, Elidrissi A & Hammouti B, *Port Electrochim Acta,* 32 (2014) 35.

30 Baumgartner L K, Reid R P, Dupraz C, Decho A W, Buckley D H, Spear J R, Przekop K M & Visscher P T, *Sediment Geol,* 185 (2006) *185*, 131.

31 Davidson D, Beheshti B & Mittelman M W, *Biofouling,* 9 (1996) 279.

32 Srimathi M, Rajalakshmi R & Subhashini S, *Arabian J Chem,* 7 (2014) 647.

33 Dittrich M & Sibler S, in *Tufas and Speleothems: Unravelling the microbial and physical controls,* Pub. 336, edited by Pedley H M, Rogerson M (The Geological Society, London) 2010, 51.

34 Gaol F L, Shrivastava K & Akhtar J, Recent trends in physics of material science and technology. Springer Series in Materials Science 204, (Springer Verlag, Singapore) 2015, 10.

35 Gunasekaran S, Sailatha E, Seshadri S & Kumaresan S, *Indian J Pure Appl Phys.* 47 (2009) 12.

36 Gunasekaran S, Seshadri S & Muthu S, *Indian J Pure Appl Phys,* 44 (2006**)** 581.

37 Sun S G, in Electrocatalysis edited by Lipkowski J & Ross P N (Wiley-VCH. Inc., New York) 1998, 243.